

Enhancing Plant Disease Identification Through Hyperspectral Imaging and AC-FNet Framework

¹Dhason Lita Pansy and ²Malaichamy Murali

¹Department of Computer Science and Engineering, SRM Institute of Science and Technology, Kattankulathur, TamilNadu, India

²Department of Computing Technologies, SRM Institute of Science and Technology, Kattankulathur, TamilNadu, India

Article history

Received: 07-03-2024

Revised: 24-09-2024

Accepted: 09-12-2024

Corresponding Author:

Dhason Lita Pansy

Department of Computer Science and Engineering, SRM Institute of Science and Technology, Kattankulathur, Tamil Nadu, India

Email: ld5358@srmist.edu.in

Abstract: The precise identification of plant diseases is essential for optimizing agricultural practices. The impact of these diseases on food production often leads to significant revenue loss. Detecting diseases that primarily manifest symptoms in plant leaves has conventionally depended on visual inspection by plant pathologists. However, modern methodologies use machine learning and computer vision techniques to facilitate disease identification, thus addressing the limitations of traditional approaches. However, in most of the existing works, the quality of the leaf image, smaller image regions, and chlorophyll content-based vegetation index features were not concentrated, which is required to be analyzed for the efficient detection of multiple leaf diseases. Therefore, this study highlights the necessity for a robust diagnostic system that tackles existing challenges in disease identification. Hyperspectral Images (HSI) serve as a valuable resource due to their rich spectral information. This research proposes a framework for multiple disease identification using hyperspectral data. The process begins by identifying target regions within the hyperspectral image through the Jeffries-Matusita-based Simple Linear Iterative Clustering (JM-SLIC) technique. Subsequently, the segmented image undergoes preprocessing, involving dead pixel replacement and noise removal. To approximate the resolution effectively, the Stochastic gradient-based Bi-cubic interpolation (S-BI) technique is employed. The resolution-approximated spectral images are then subjected to unmixing, followed by the estimation of chlorophyll content-based indexes. These indexes, combined with various features, contribute to disease identification within the leaf using the Atrous Convolution-based FractalNet (AC-FNet) model. The experimental outcomes strongly support the effectiveness of the proposed framework in detecting plant diseases efficiently.

Keywords: Atrous Convolution-Based FractalNet (AC-FNet), Hyper-Spectral Image (HSI), Vegetation Index (VI), Stochastic Gradient-Based Bi-Cubic Interpolation (S-BI)

Introduction

Plant diseases significantly impact agricultural yield, which poses a challenge to farm efficiency (Görlich *et al.*, 2021). Effective disease management is important for sustaining crop productivity and minimizing losses (Abade *et al.*, 2021). However, detecting and managing plant diseases present ongoing challenges, especially with the emergence of new diseases in previously unaffected areas (Chakraborty *et al.*, 2021). Diseases affecting plants can vary in type and can target different plant organs. Early symptoms of many plant diseases often manifest on

leaves, thus allowing for identification through visual inspection (Ahmad *et al.*, 2023). Additionally, the color variations in leaves directly relate to changes in chlorophyll content, which serves as an informative indicator of plant health (Gao *et al.*, 2021; Hua *et al.*, 2022). Therefore, analyzing chlorophyll content plays an essential role in predicting and diagnosing leaf diseases.

Currently, assessing chlorophyll content depends on UV spectrophotometry and fluorescence analysis, but these methods are notably inefficient (Qi *et al.*, 2021). The traditional approach that is reliant on expert opinion is time-consuming and sometimes impractical (Ngugi *et al.*,

2021). As an alternative, Hyperspectral Imaging (HSI) emerges as a non-destructive technique for early crop disease detection, enhancing both spatial and spectral image data (Lay *et al.*, 2023). HSI facilitates the prediction of diseases even before visible symptoms emerge (Ouhami *et al.*, 2021). Prior research has employed HSI in plant disease detection using various techniques, such as Vegetation Indices (VIs) and machine learning approaches like Artificial Neural Networks (ANN) (Shahi *et al.*, 2023). However, most studies have concentrated on identifying single diseases like white leaf disease in sugarcane (Zamani *et al.*, 2022), potato late blight (Kundu *et al.*, 2021), and similar singular diseases. Notably, these models struggled to detect multiple diseases affecting a single plant. To address this limitation, this article proposes a method for multi-disease prediction in multiple plants.

Research Motivation

Even though many research studies related to leaf disease were delivered by different authors, some specific limitations restricted the superiority of the prediction outcome. In most of the prevailing leaf disease prediction systems, the gathered leaf images were not preprocessed efficiently. This led to the training of the noisy and imperfect image data, causing incorrect disease prediction. Furthermore, the image resolution played a significant role in detecting the leaf diseases, which were not analyzed deeply in the existing works. Also, the existing works processed the leaf images either based on the image features or the vegetation index features, which does not exactly outlet the leaf disease. Additionally, the efficiency of the prediction model also impacted the accuracy of the prediction. But, in most of the conventional works, the overfitting or gradient vanishing issue of the classifier degraded the detection performance. Hence, these drawbacks, which are probably found in the related works, remain the motivation behind the proposed work for developing the enhanced detection of multiple diseases in plant leaves.

Problem Statements

Current approaches in plant disease prediction utilizing Hyperspectral Imaging (HSI) cause several limitations:

- Even though HSI achieved better accuracy for single disease prediction in plants, the multi-disease identification within multiple plants was not effectively concentrated by HSI in existing works (Mahum *et al.*, 2023)
- Disease prediction based on low-resolution leaf images and post-separation from soil images diminishes prediction accuracy (Liao *et al.*, 2022)
- Leaf disease predicted solely through indexes without considering leaf features caused unreliable prediction outcomes (Rahman *et al.*, 2023)

Major Contributions

By addressing the aforementioned issues, the novel contributions of the proposed model are as follows:

- The AC-FNet model is utilized to develop an efficient leaf disease prediction model capable of handling multiple disease scenarios in multiple plants. With the help of this utilized model, the low-level feature maps of leaf images are rapidly processed and efficiently predict diseases
- The resolution of leaf images is enhanced by introducing the S-BI technique for accurate disease classification
- To improve the prediction accuracy for multi-disease occurrences in individual plants, both disease and leaf features are incorporated along with the indexes. Hence, the leaf structure gets deeply analyzed and the diseases are exactly predicted.

Related Work

Tetila *et al.* (2020) proposed the use of Deep Convolutional Neural Networks (DCNN) to identify soybean leaf diseases in UAV images. The approach employed SLIC segmentation for leaf separation, which shows higher accuracy in disease prediction with DCNN. However, the post-SLIC segmentation caused lower-resolution images, potentially affecting the result's reliability. Liao *et al.* (2022) introduced a model for Eucalyptus leaf disease detection using UAV multispectral Imagery. The approach utilized random forests for disease prediction. Also, incorporating spectral bands and VIs with the approach enhanced model accuracy. However, the absence of proper dead pixel calibration could degrade the random forest's outcomes. Wang *et al.* (2022) advocated a convolution network enhanced transformer for classifying tomato diseases that depended on a vision transformer. Results indicated the model's reliability and accuracy. But, the visual transformer, with a limited dataset, was susceptible to overfitting.

Lei *et al.* (2021) presented a method for remote sensing detection of Yellow Leaf Disease (YLD) in Areca nut. The scheme employed five VIs and five classifier models, thus achieving higher accuracy in YLD severity prediction. However, image noise negatively impacted the results. Du *et al.* (2023) proposed a strategy for monitoring Wheat Stripe Rust (WSR) using Sun-Induced chlorophyll Fluorescence (SIF) and NDVI to predict WSR severity levels. While they attained higher WSR severity prediction, the approach's accuracy was influenced by phenological differences. Ashwini and Sellam (2023) utilized Ebola Optimization Search (EOS)-based 3-D dense CNN for accurate corn leaf disease prediction. The EOS technique reduced classification errors, ensuring precise disease prediction. Srivastava *et al.* (2021)

conducted a sensitivity analysis of ANN for chlorophyll prediction, employing the Leks' profile method. The outcomes highlighted chlorophyll's role in predicting crop health status. However, the leaf structure was not analyzed, which resulted in inaccurate disease prediction.

Materials and Methods

This section aims to outline the materials and equipment incorporated in this research for plant disease identification using hyperspectral imaging and the AC-FNet approach. The hyperspectral images are acquired using a Hyperspectral Imaging (HSI) camera, covering a spectral range [400-1000 nm] with a spectral resolution of [5 nm]. The imaging system is configured to acquire plant leaf samples under controlled illumination using halogen/tungsten light sources. Also, the proposed work utilizes the publically available hyperspectral plant disease dataset named plant village-HSI dataset. Moreover, the proposed method introduces the JM-SLIC to isolate target regions effectively. Further, the proposed S-BI method is used to improve the spatial resolution of hyperspectral images. This section ensures reproducibility and transparency of the research by providing significant details about the materials.

Detecting multiple diseases in plants before visible symptoms emerge can significantly enhance plant yield. Therefore, this study proposes a multi-disease prediction model using AC-FNet for multiple plants, as depicted in Fig. (1).

Input Data

Initially, the input HSI of tomato, corn, soybean, and mango crops taken by the Unmanned Ariel Vehicle (UAV) is denoted as:

$$L_n = \{L_1, L_2, \dots, L_\alpha\} \quad (1)$$

where, L_α signifies the α^{th} leaf image.

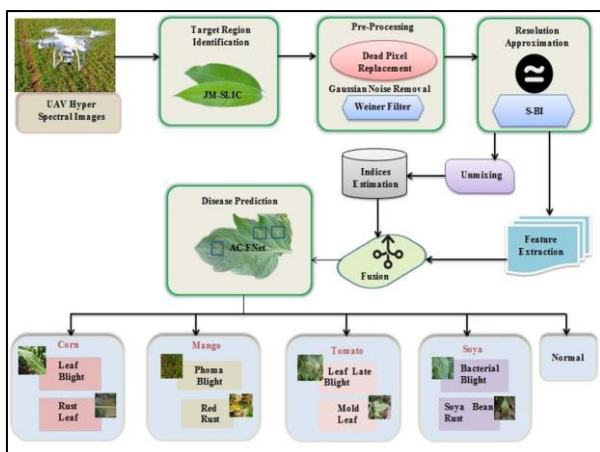


Fig. 1: Architecture of the proposed model

Target Region Identification

The images captured by UAVs include the field area along with the leaves, thus necessitating separate segmentation of leaf images. This segmentation is achieved using the Jeffries Matusita-based Simple Linear Iterative Clustering (JM-SLIC) technique. While SLIC generates compact superpixels efficiently, its time complexity poses limitations. To address this, the Jeffries Matusita (JM) technique is incorporated within SLIC, which also reduces the computational challenge. Initially, the Hyperspectral Image (HSI) undergoes uniform segmentation into superpixels based on the total pixel count blocks of the same size as P/K .

Then, the characteristic vector of the center of the superpixel block z is given as:

$$c_z = [\ell_z, a_z, b_z, u_z, v_z] \quad (2)$$

Here, ℓ, a, b denotes the color values of lab space, and u, v represents the coordinates of the pixel. Each center point contains a specific label and the distance is calculated to the neighboring superpixel blocks using JM as:

$$\mathfrak{R}_{lab} = \sqrt{(\ell_{z+1} - \ell_z)^2 + (a_{z+1} - a_z)^2 + (b_{z+1} - b_z)^2} \quad (3)$$

$$\mathfrak{R}_{uv} = \sqrt{(u_{z+1} - u_z)^2 + (v_{z+1} - v_z)^2} \quad (4)$$

$$d_z = 2(1 - \exp(\mathfrak{R}_{lab} + \frac{\beta}{C} \mathfrak{R}_{uv})) \quad (5)$$

where, \mathfrak{R}_{lab} and \mathfrak{R}_{uv} are the color and space differences between pixels, respectively, d_z is the similarity degree between pixels, C is the center point distance and β is the balance parameter to control the compactness of superpixel blocks after clustering. For smaller d_z , the pixels are assigned with the same label as c_z . Once all the superpixels are grouped, the center point (ϕ) of the blocky is re-calculated as:

$$\phi_y = \frac{1}{P_y} \sum c_\delta \quad (6)$$

where, c_δ is the 5-dimensional characteristic vector of the pixel u_δ in the superpixel clustering region, the process is iterated until all the pixels are converged.

Then, the adjacent merging strategy is used to eliminate the isolated pixels with small sizes to ensure the connectivity of the final obtained target images. The final obtained target images are given as follows:

$$l_q = \{l_1, l_2, \dots, l_\varepsilon\} \quad (7)$$

where, l_ε depicts the ε^{th} leaf image obtained after the JM-SLIC segmentation.

Preprocessing

For the extracted leaf image l_q , preprocessing is performed to enhance the accuracy of the disease prediction.

Dead Pixel Removal

Dead pixels refer to missing or zero-valued pixels within the Hyperspectral Image (HSI). In this context, pixels that contain 25% zero values within the spectrum are identified as dead pixels. These pixels are substituted by computing the median values from neighboring pixels.

Gaussian Noise Removal

Once the dead pixels are removed, the Gaussian noise is removed using the Weiner filter ($F(l_q)$) as:

$$F(l_q) = \frac{B^*(u,v) \cdot p_m(u,v)}{|B(u,v)|^2 \cdot p_m(u,v) + A(u,v)} \quad (8)$$

where, $p_m(u, v)$ is the images' power spectra, $A(u, v)$ is additive noise, the blurring filter is denoted as $B(u, v)$ and $B^*(u, v)$ depicts the inverse filtering.

Thus, the preprocessed image is given as λ_q .

Resolution Approximation

After preprocessing, the image resolution is improved using the S-BI technique to address the low-resolution images generated by JM-SLIC. Bi-cubic Interpolation is chosen for its effective magnification and sharpening capabilities. However, precise edge interpolation may be compromised due to neighboring pixel calculations. To mitigate this, a stochastic gradient is included within the BI technique to enhance edge accuracy.

The S-BI uses an up-sampling distance U to estimate the unknown pixels for interpolation.

At a pixel position (j, k) , the pixels are interpolated as:

$$I_{j,k}^{\wedge} = [\varpi_{-1}(U_\lambda) \ \varpi_0(U_\lambda) \ \varpi_1(U_\lambda) \ \varpi_2(U_\lambda)] \begin{bmatrix} I_{j-1,k-1} & I_{j,k-1} & I_{j+1,k-1} & I_{j+2,k-1} \\ I_{j-1,k} & I_{j,k} & I_{j+1,k} & I_{j+2,k} \\ I_{j-1,k+1} & I_{j,k+1} & I_{j+1,k+1} & I_{j+2,k+1} \\ I_{j-1,k+2} & I_{j,k+2} & I_{j+1,k+2} & I_{j+2,k+2} \end{bmatrix} \begin{bmatrix} \varpi_{-1}(U_\mu) \\ \varpi_0(U_\mu) \\ \varpi_1(U_\mu) \\ \varpi_2(U_\mu) \end{bmatrix} \quad (9)$$

Here, $U_\mu = k - k$, $U_\mu = j - j$, and $I_{j,k}$, are the pixels at the position (j, k) , and $\varpi_{-1}, \varpi_0, \varpi_1, \varpi_2$ are the weights of S-BI, which are calculated as:

$$\left. \begin{aligned} \varpi_{-1}(U, G) &= \frac{-U^3 + 2U^2 - U}{2}, G \\ \varpi_0(U, G) &= \frac{3U^3 + 5U^2 + 2}{2}, G \\ \varpi_{-1}(U, G) &= \frac{-3U^3 + 4U^2 - U}{2}, G \\ \varpi_{-1}(U, G) &= \frac{U^3 - U^2}{2}, G \end{aligned} \right\} \quad (10)$$

where, G represents the stochastic gradient of the interpolated pixel to the neighboring pixels, which is equated as:

$$G = \phi_k - \eta \left(\frac{\partial}{\partial \phi_j} \cdot Q(\phi_j) \right) \quad (11)$$

Here, $Q()$ is the summed gradient value of the neighboring pixels and ϕ_k is the gradient between the pixel position k and k . η is the parameter for controlling the gradient of the interpolated pixel. Thus, the resolution-enhanced image (R_q) is obtained.

Un-Mixing

As the enhanced HSI image R_q contains red, blue, Near Infra-Red (NIR), and green spectral bands, they are separated with an un-mixing technique for easier computation of the VIs. Here, the Bayesian method is used for un-mixing based on the posterior probability density ($\rho(\Phi, \omega | R, \theta)$) as:

$$\rho(\Phi, \omega | R, \theta) = \frac{\rho(R | \Phi, \omega, \sigma^2) \cdot \rho(\Phi | \theta) \rho(\omega | \theta) \rho(\sigma^2 | \theta)}{\rho(R)} \quad (12)$$

where, σ, Φ, ω represent the parameters of the probability distribution, θ is a super parameter made up of σ, Φ, ω . $\rho(R | \Phi, \omega, \sigma^2)$ denotes the likelihood function and $\rho(\Phi | \theta), \rho(\omega | \theta), \rho(\sigma^2 | \theta)$ are the prior distribution of end-members, abundance, and noise, respectively. Thus, the spectral set is depicted as s .

Indices Estimation

From s , the chlorophyll content-based VI features, such as Normalised Difference VI (NDVI), Green NDVI (GNDVI), Red-Green Ratio (RGR), Infrared Percentage VI (IPVI), Green Chlorophyll Index (CL_{green}), red-edge Chlorophyll Index ($Cl_{rededge}$) and Chlorophyll VI (CVI) are estimated. The dimensions of the retrieved indices-based leaf features are 1'7. Thus, the obtained VI set is depicted as $V_h, h = 1, 2, \dots, 7$.

Feature Extraction

Meanwhile, to predict the multi-disease in a single leaf, image-based features like airspace characteristics (S), texture features (T), and Sequential Maximum Angle Convex Cone (SMACC) (E) features are extracted as:

$$\left. \begin{aligned} S &= \int dg_1 / dg_2 \\ T &= GF \\ E &= \sum_{\vartheta=1}^W Y(i, \vartheta) N(\vartheta, v) \end{aligned} \right\} \quad (13)$$

where, g_1 and g_2 are the green and non-green pixels, respectively, GF denotes Gray Level Co-occurrence Matrix (GLCM) features, such as mean, dissimilarity, homogeneity, contrast, second moment, and entropy, i depicts the band index, W signifies the total number of end members, N is the abundance of end-member v to end-member ϑ and Y is the end-member spectrum matrix. The extracted image-based features from the leaf image are in the dimension of 1'14. The final feature set is given as H_3 .

Feature Fusion

Then, to combine the VI features and the image features, the feature fusion for the single leaf takes place, which is described as:

$$\lambda_q = H_{\mathfrak{N}} \cup V_h \quad (14)$$

Here, λ_q depicts the fused feature set of the leaf q and \cup symbolizes the combining or fusing operation, which unites both the indices-based leaf features and the image-based features. So, the fused feature vector has a dimension of 1'21. This fused dimension of the feature vector is minimized to 1'10 based on the dimension reduction approach. Thus, the dimensionality curse problem is prevented without losing information. Thus, λ_q with reduced dimension is mentioned as τ_q and is subjected to further processing.

Disease Prediction

Then, the τ_q is given to the AC-FNet for single and multi-leaf disease prediction.

FractalNet predicts the results with less error. However, the low-level mapping of the feature increases the prediction time with the normal convolution in FNet. So, Atrous convolution is used in the FNet. The architecture of FNet is given in Fig. (2).

For training the fused features of leaf images, the hyperparameters include depth or levels of the network, number of neurons, number of recursive steps, activation function, learning rate, batch size, weights, and biases, which are considered in the proposed AC-FNet model. By adjusting these hyperparameters, the desired outcome is returned by the proposed classifier. The process of the proposed AC-FNet for leaf disease prediction is explained as follows.

Atrous convolution: The input τ_q is passed through multiple fractal blocks to produce the output disease class. Here, the receptive fields are widened by the Atrous convolution, and the data are learned more efficiently through the kernel function. The process in the fractal block ν with the input is specified as ζ and is defined based on the $AC(e(\cdot))$ as:

$$e_1(\zeta) = \sum(\zeta) * \Gamma(K(\gamma)) \quad (15)$$

Here, $*$ Γ depicts the dilated convolution and $K(\gamma)$ defines the kernel function. Then, the successive fractals ($\aleph_{\xi+1}(\zeta)$) are defined through the join operations. It is expressed as:

$$\aleph_{\xi+1}(\zeta) = [(\aleph_{\xi} \circ \aleph_{\xi})(\zeta)]\theta[e_{nn}(\zeta)] \quad (16)$$

where, \circ , θ denotes the composition and join operations, ξ is the index of the truncated fractal $\aleph_{\xi}(\cdot)$ and θ merges the two feature blobs into one.

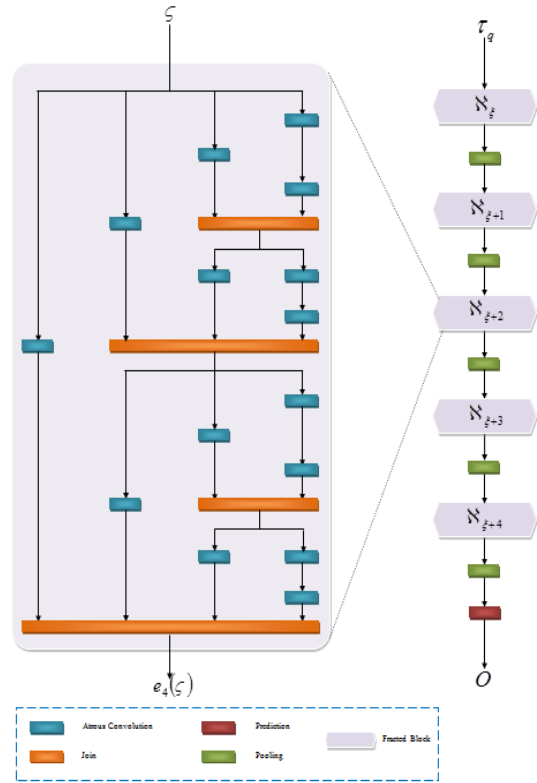


Fig. 2: AC-FNet

Pooling: Then, the max-pooling process (X_{pool}) is performed to process the feature maps as:

$$X_{pool} = \nabla \left[\frac{\aleph_{\xi+1}(\zeta) + 2\varphi - K}{\psi} \right] + 1 \quad (17)$$

where, φ and ψ are the padding and stride size, respectively, and $\nabla(\cdot)$ depicts the rectified linear unit. Finally, the prediction layer predicts the output (O) after batch normalization as:

$$O = \frac{1}{\xi} \sum X_{pool} \quad (18)$$

where, ξ depicts the number of layers.

Loss function: Finally, the loss function, namely weighted cross-entropy loss (ω_{loss}) (Hossain *et al.*, 2023), is calculated to minimize the deviation between the predicted disease classes (O) and the actual disease class (α). Here, the weighted cross entropy loss function is utilized to handle the variation between the actual and predicted classes. By doing so, the class of the leaf images is properly estimated regardless of the majority and minority of the features, thus enhancing the multi-class classification of leaf diseases. The ω_{loss} is analytically evaluated as:

$$\omega_{loss} = -\frac{1}{d} \sum_{i=1}^d \sum_{n=1}^N w_n \times O \log(\rho(O \approx \alpha)) \quad (19)$$

where, d denotes the number of input samples, w_n indicates the weights of the number of disease classes, ρ represents the probability of $O \in \alpha$ and \log denotes the logarithmic function. The training of the proposed AC-FNet is iterated (I) until the minimum variation between the predicted and target class is achieved. Otherwise, the hyperparameters of the model are adjusted and the training is repeated until maximum iteration (I_{Max}). Hence, the various disease classes of the plant leaves are predicted using the proposed model. The pseudocode of AC-FNet is,

Input: Fused features
Output: Predicted disease

Begin

Initialize the number of layers, fractal blocks $\aleph_{\xi+1}, \psi, K, \varphi$, maximum accuracy Z_{max}

For each τ_q

If predicted accuracy ($X_{acc} \geq Z_{acc}$) {

Return output O

} **Else** {

Update kernel

Compute fractal blocks $\aleph_{\xi+1}(\zeta)$

Perform $* \Gamma$

Obtain output after X_{pool}

}

End If

Calculate the Loss function, $\overline{\omega}_{loss}$

End for

$I \rightarrow I_{Max}$

Return O

End

Here, AC-FNet predicts corn leaf blight, corn leaf rust, mango phoma blight, mango red rust, tomato leaf late blight, tomato leaf mold, soybean rust, soybean bacterial blight diseases, and normal healthy leaf classes. Also, AC-FNet predicts multiple diseases in a single leaf.

Downsides of the Proposed Model

Even though all the information on leaf regions is effectively learned by the proposed method, it has some limitations. The proposed model requires prolonged training and causes computational complexity due to the processing of multiple neuron layers.

Results

This section comparatively analyzes the performance of the proposed model through the experimental results implemented on the MATLAB platform. The dataset used for experimentation is sourced from publicly available sources. The visual representation of sample image outcomes is illustrated in Fig. (3).

Dataset Description

To evaluate the performance of the proposed methodology, the hyperspectral images of leaf diseases are gathered from the Plant Village dataset. This dataset contains 20,600 leaf disease images, including Early blight, late blight, bacterial spot, Rust and leaf mold, along with the healthy leaf images of different plants. Among them, 80% of the data (16480 images) is used for training and 20% of the data (4120 images) is used for testing the proposed method.

Experimental Setup

For executing the proposed model, the MATLAB working platform of version 2022a, which was developed by MathWorks, is used. This platform is specifically designed to make faster and easier scientific calculations. Also, this programming tool has the ability to call external libraries, which evolve applications with the graphics user interface. By using the MATLAB platform, different applications, including matrix manipulations, plotting of functions and data, algorithms implementation, user interface creation, and interfacing with other programming languages, such as C, C++, C#, Java, Fortran, and Python, are efficiently performed. The configurations of the machine defined for performance analysis are mentioned as follows:

- Processor: Intel core i5
- CPU speed: 3.30 GHz
- Operating system: Windows 10
- Random Access Memory (RAM): 8 GB



Fig. 3: (a) Input image, (b) Target region identification, (c) Noise removal image, and (d) Image resolution

Performance Analysis

In this section, the effectiveness of the proposed algorithms is empirically demonstrated by comparing them with the existing techniques through the different performance metrics and evaluation matrices. As every process contributes to the overall efficiency of the proposed system, the performance is assessed for each critical process in the proposed leaf disease detection model.

Evaluation Performance of Target Region Segmentation

Table (3) and Fig (8) reveal that for the target region segmentation, the JM-SLIC technique dominated the SLIC, Density-Based Spatial Clustering of Applications with Noise (DBSCAN), Fuzzy-C-Means (FCM) and k-means algorithms by attaining the least TRIT of 672ms.

Performance Analysis of Pixel Resolution Approximation

Table (2) presents the SSIM, RAT, and PSNR comparisons between the proposed S-BI method and existing techniques like Directional Cubic Convolution Interpolation (DCCI), Iterative Curvature-Based Interpolation (ICBI), and Bi-Linear Interpolation (BLI). The S-BI algorithm yields an SSIM of 0.9634 and an RAT of 1.7ms.

Figure (7) reveals that the SSIM, RAT, and PSNR of the BI are higher than the other traditional techniques. However, the S-BI attained higher quality results with a PSNR value of 35.26 dB.

Performance Assessment of Leaf Disease Identification

The findings depicted in Fig. (4) validate that the proposed AC-FNet achieved a superior recognition rate of 98.79% than existing methods like FNet, Residual-Network (ResNet), DCNN, and ANN. Additionally, the AC-FNet exhibited higher specificity, recall, precision, and f-measure metrics than the existing techniques.

Table (1) reveals that the proposed AC-FNet obtained a lesser prediction time (13675) compared to the existing FNet and ANN techniques. Similarly, the proposed method achieves 0.0761% FNR and 0.0673% FPR.

The results depicted in Fig (5) show the Area Under the Curve (AUC) values, which indicate the accurate prediction rates achieved by both the proposed and existing models. The proposed AC-FNet demonstrates an AUC value of 0.98, thus surpassing the AUC values of Fnet (0.96) and ResNet (0.94).

Table 1: Prediction time results

Techniques	Prediction time (ms)	FNR (%)	FPR (%)
Proposed AC-FNet	13675	0.0761	0.0673
FNet	27643	0.094	0.0842
ResNet	38435	0.1068	0.1043
DCNN	57614	0.1267	0.1375
ANN	69426	0.1573	0.1504

Table 2: Results for SSIM, RAT and PSNR

Techniques	SSIM	RAT (ms)	PSNR (DB)
Proposed S-BI	0.9634	1.7	35.26
BI	0.9472	4.6	33.05
DCCI	0.9261	9.7	31.86
ICBI	0.9001	12.3	30.75
BLI	0.8837	16.7	28.19

Table 3: Target Region Identification Time (TRIT) values

Techniques	TRIT (ms)
Proposed JM-SLIC	672
SLIC	861
DBSCAN	1076
FCM	1243
K-Means	1407

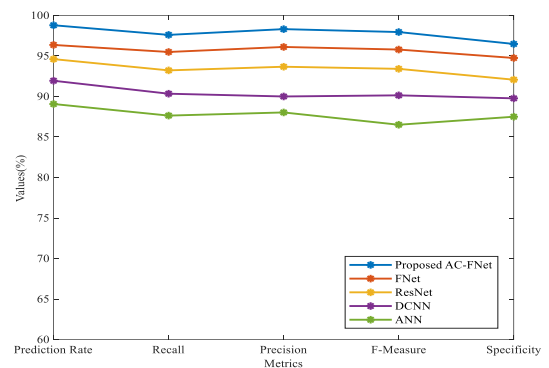


Fig. 4: Performance analysis recognition rate

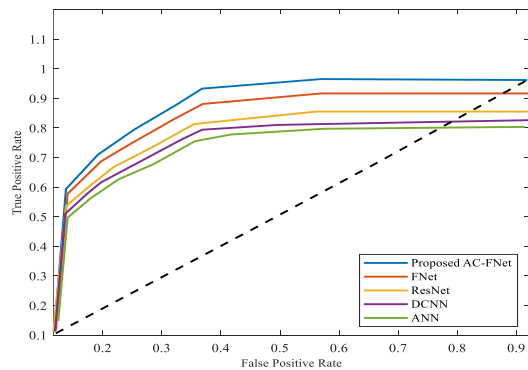


Fig. 5: AUC analysis

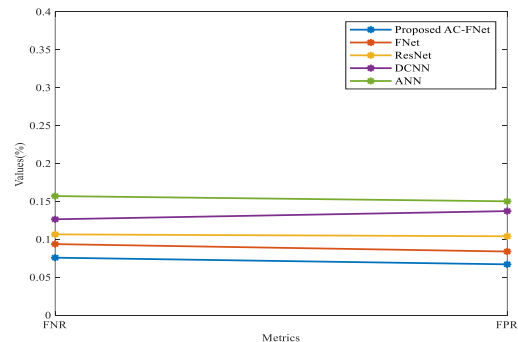


Fig. 6: FNR and FPR analysis

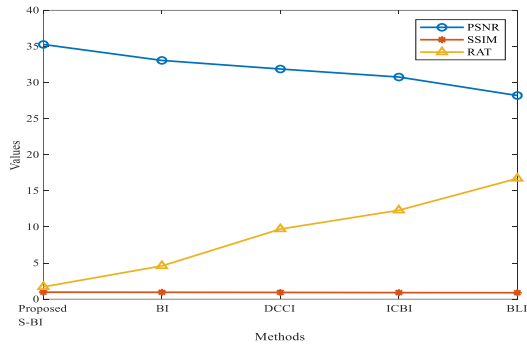


Fig. 7: Analysis of SSIM, RAT, and PSNR

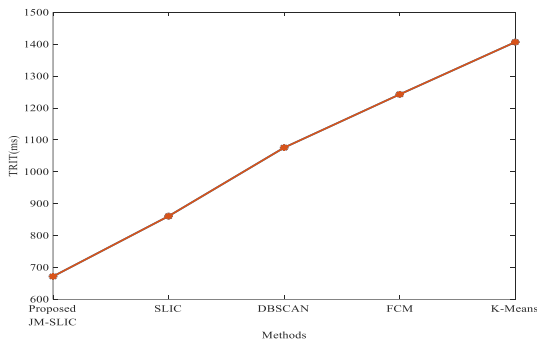


Fig. 8: TRIT analysis

Figure (6) reveals that the FNR and FPR of the traditional prediction models are higher than the proposed AC-FNet. The AC-FNet attained low FNR (0.0761) and FPR (0.0673), even for the multi-disease prediction also. This proves that the disease prediction was performed with less error, with the AC-FNet only.

The leaf disease classification by the proposed method is analyzed in Table (4) with respect to Mean Square Error (MSE), Mean Absolute Error (MAE), and Root Mean Square Error (RMSE). Here, the existing FNet attained 2.315 MSE, ResNet attained 0.516 of MAE and ANN attained 2.123 of RMSE, which are higher than the developed model. The proposed AC-FNet obtained a lower MSE, MAE, and RMSE of 1.031, 0.125, and 1.015, respectively.

Statistical Analysis

Here, the proposed model for plant leaf disease detection is assessed in terms of statistical measures, such as Mean accuracy, variance, and Standard Deviation (SD) for different epochs by comparing it with the state-of-art methods.

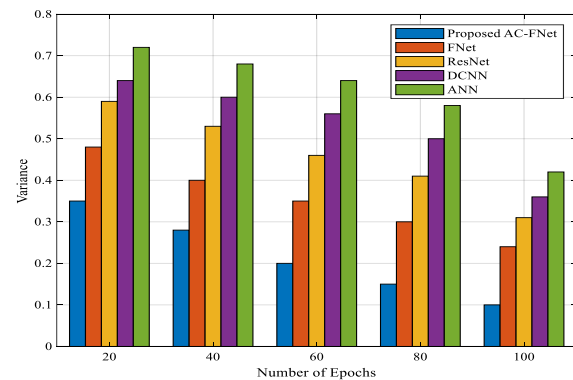
The performance of the proposed method over the existing methods is evaluated in terms of mean accuracy and is represented in Table (5). The mean accuracy of the model increases with the increasing number of epochs. Here, the proposed model attained 98.79% mean accuracy for 100 epochs, which is reduced to 93.68% for 20 epochs. In the meantime, for 100 epochs, the existing FNet and DCNN attained lower mean accuracy of 96.54% and 92.86%, respectively.

Table 4: Error analysis of the proposed model

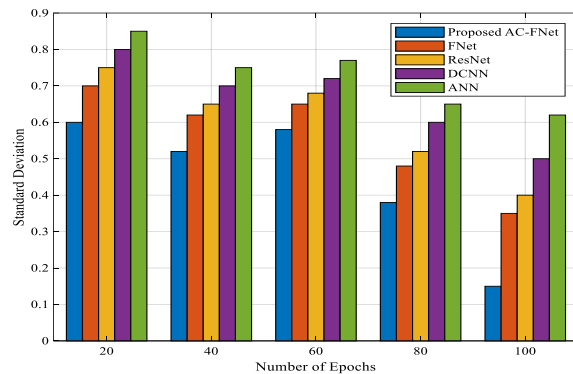
Methods	MAP	MAE	RMSE
Proposed AC-FNet	1.031	0.125	1.015
FNet	2.315	0.372	1.521
ResNet	2.847	0.516	1.687
DCNN	3.294	0.593	1.814
ANN	4.508	0.640	2.123

Table 5: Evaluation of mean accuracy

Methods	Mean accuracy (%)				
	No. of Epochs				
	20	40	60	80	100
Proposed					
AC-FNet	93.68	94.10	95.48	97.25	98.79
FNet	92.16	93.30	94.71	96.02	96.54
ResNet	91.57	92.84	93.56	94.92	95.47
DCNN	88.37	89.56	90.44	91.75	92.86
ANN	87.24	87.69	88.03	88.60	89.83



(a)



(b)

Fig. 9: Illustration of statistical analysis; (a) Comparison Performance regarding variance; (b) SD evaluation

Figure (9 a-b) represents the statistical outcome of the proposed technique with respect to variance and SD. The proposed model achieved minimum SD and variance of 0.14 and 0.02, respectively, for the maximum epochs. Meanwhile, for 100 epochs, the existing methods, namely ResNet, attained a Variance of 0.26 and SD of 0.50 and ANN attained 0.37 and 0.61 variance and SD, as in Fig. (9 a-b), respectively.

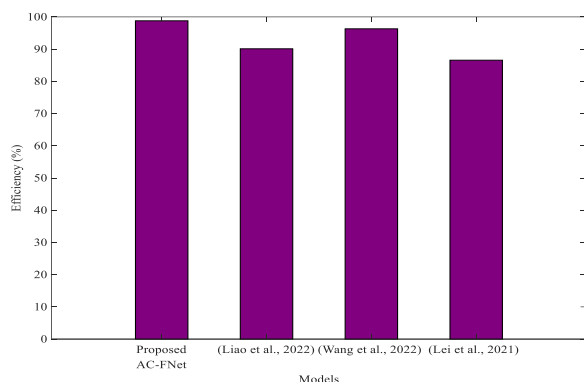


Fig. 10: Comparative analysis model

Comparative Analysis

In this section, the proposed AC-FNet is comparatively analyzed with the existing (Liao *et al.*, 2022; Wang *et al.*, 2022; Lei *et al.*, 2021) models.

Figure (10) shows the superior efficiency in disease recognition accuracy exhibited by the proposed model compared to existing ones. Specifically, in single-leaf disease recognition, the models from (Liao *et al.*, 2022; Wang *et al.*, 2022; Lei *et al.*, 2021) achieved accuracies of 8.69, 2.49 and 12.22%, respectively, which are lower than the proposed model. Moreover, the proposed model for leaf disease detection is analogized with recent works, including (Rahman *et al.*, 2023; Javidan *et al.*, 2024 and Mahum *et al.*, 2023) in terms of prediction accuracy.

Table (6) exhibits the performance of the proposed method regarding prediction accuracy by comparing it with the recent studies of leaf disease detection. The proposed model obtained a higher accuracy of 98.79%. At the same time, the existing methods (Rahman *et al.*, 2023; Javidan *et al.*, 2024; Mahum *et al.*, 2023) attained prediction accuracy of 95.00, 95.58 and 97.20%, respectively, which are lower than the proposed model.

Discussion

This section aims to interpret and discuss the results of the proposed work. To validate the performance of the proposed work, the findings of the proposed approach are compared with several existing techniques regarding various quality factors. The performance analysis is done regarding target region segmentation, pixel resolution approximation, and leaf disease identification. Primarily, the target regions, identified from the input data using the proposed JM-SLIC method, are analyzed in terms of Target Region Identification Time (TRIT) by comparing it with the prevailing methods. The proposed JM-SLIC technique obtained minimum TRIT, ensuring the efficiency of target region segmentation. Further, the pixel

resolution, which is approximated by using the proposed S-BI technique to attain the accurate disease classification, is analyzed based on Structural Similarity Index Metric (SSIM), Resolution Approximation Time (RAT), and Peak Signal to Noise Ratio (PSNR). For pixel resolution approximation, the proposed S-BI technique performs better than the developed algorithms. Thus, the findings validate the ability of the S-BI technique to effectively preserve leaf structure. Further, the analysis outcomes proved that the S-BI technique provided better resolution.

In the same manner, the leaf disease classified using the proposed AC-FNet model is analyzed in terms of various metrics, namely recognition rate or accuracy, Prediction time, False Negative Rate (FNR), False Positive Rate (FPR), and Area Under the Curve (AUC). To verify the efficiency of the proposed model, the performance is evaluated by comparing it with the existing techniques, which already performed a similar prediction task. The improved outcomes in both single and multiple-leaf detections can be attributed to the resolution approximation within the identified target regions. Thus, the analysis shows the suitability of the proposed model for effective multi-disease prediction in plant crops. Due to the incorporation of AC, the proposed AC-FNet achieved minimum prediction time. This demonstrates the time efficiency achieved by the proposed algorithm. Moreover, the proposed AC-FNet obtained lower FPR and FNR than the existing networks. Likewise, the AUC analysis proves that AC-FNet adeptly predicts both diseased and healthy leaves.

The traditional methods attained sub-optimal outcomes with more error due to insufficient quality and feature analysis performed on the leaf images. However, the proposed method classified the leaf diseases by focusing on the target regions, preprocessing, pixel resolution, chlorophyll content-based VI indices, and image features. Additionally, the fusing of both the indices and image features with reduced dimension prior to the training aids in classifying the leaf diseases with lower MSE, MAE, and RMSE. Hence, the performance of the proposed technique is enhanced by negligible error compared to the existing techniques. As the proposed network analyzed the low-level mapping of the features without the inclusion of additional parameters, it better predicted leaf diseases than the other methods. Thus, the performance of the proposed model is enhanced than the existing techniques. Also, the statistical analysis is carried out in the proposed work. Generally, the lower values of the variance and SD among the data depict the improved efficiency of the model. The proposed work had impressive performance due to the unmixing of spectral bands and the feature fusion processes carried out prior to training. Overall, it is observed that the statistical performance is improved using the proposed technique over the other prevalent techniques.

Table 6: Comparative analysis model with recent work

Authors	Technique used	Prediction accuracy (%)
Proposed	AC-FNet	98.79
(Rahman <i>et al.</i> , 2023)	Support Vector Machine (SVM)	95.00
(Javidan <i>et al.</i> , 2024)	Weighted ensemble learning	95.58
(Mahum <i>et al.</i> , 2023)	DenseNet 201	97.20

To prove the model's significance, the proposed work is compared with the prevailing state-of-the-art works. The comparative analysis (Table 6) proved the better efficiency of the proposed work. As the low-level features are effectively captured by the dilated convolution form of the utilized Atrous convolution, the proposed model predicted leaf disease with a higher accuracy. Since the low-quality images are trained without analyzing the VI-based leaf features, the existing techniques produced lesser prediction accuracy. Hence, these results underscore the enhanced leaf disease prediction efficiency achieved by the proposed model. Thus, the comparative analysis exhibited that the proposed work had better results than prior frameworks.

Practical Applications and Limitations

By deploying the proposed model in real-time applications, the leaf diseases will be deeply analyzed based on their vegetation indices and leaf image features. So, the farmers' intervention in detecting the leaf nature with the naked eye and the difficulties behind the direct investigation are neglected. Further, the leaf diseases from the farmers' crops are more accurately predicted by the proposed model. This aids in controlling the spread of leaf disease through the incorporation of necessary pesticides and fungicides in advance to improve crop production and food security. However, some notable limitations occurred while localizing the proposed model in practical life. The DL-based proposed network requires higher computational resources with super-efficient hardware setup, expanded storage space, and prolonged time consumption for training. It also requires proper maintenance to consistently deliver accurate predictions. Moreover, the farmers are not very aware of these advanced techniques; thus, prior teaching about the model should be presented to them.

Conclusion

This article introduces an AC-FNet-based approach for multi-leaf disease prediction within UAV hyperspectral images. To identify target regions and enhance resolution, novel techniques like JM-SLIC and S-BI are proposed and subsequently evaluated against existing methods. The AC-FNet model achieved a remarkable recognition rate of 98.79% for both single and multiple disease predictions. Additionally, JM-SLIC efficiently identified target regions within a shorter duration of 672ms. Moreover, the PSNR and SSIM metrics confirmed the effectiveness of S-BI.

Future Work

Although the plant diseases are efficiently detected by the proposed model, the limitation arises when inexperienced farmers interpret leaf diseases in real-time. To address this, future work will integrate the IoT edge technology with the proposed model to store and retrieve disease information. By using IoT technology, the sensor devices in the form of sensor cameras are deployed to examine the leaf structure. These sensors will regularly capture the characteristics of the leaf, including the leaf color, texture, and other significant factors. Further, the sensor-collected leaf information is transmitted through any communication protocols, such as Wireless-Fidelity (Wi-Fi), Zigbee, Low Power Wide Area Networking (LPWAN), and so on. Afterwards, the collected information is applied to the proposed model and the leaf diseases are predicted based on the trained database. This integration could facilitate easier access and comprehension of predicted diseases for budding farmers. Hence, leaf diseases are identified in real-time by continuous monitoring of plant leaves through IoT-based sensor devices. Thus, the farmers proceed to ensure the plant's health and stimulate crop production.

Acknowledgment

We thank the anonymous referees for their useful suggestions.

Funding Information

This study has no funding resources.

Author's Contributions

Dhason Lita Pansy: The first draft of the manuscript, contributed to the study conception and design. Material preparation, data collection, and analysis were performed.

Malaichamy Murali: Contributed to the study conception and design.

Ethics

This article does not contain any studies with human participants or animals performed by any of the authors.

Conflict of Interest

The authors declare that they have no conflict of interest.

Availability of Data and Materials

Data sharing is not applicable to this article as no datasets were generated or analyzed during the current study.

Competing Interests

The authors have no competing interests to declare that are relevant to the content of this article.

References

- Abade, A., Ferreira, P. A., & de Barros Vidal, F. (2021). Plant Diseases Recognition on Images Using Convolutional Neural Networks: A Systematic Review. *Computers and Electronics in Agriculture*, 185, 106125. <https://doi.org/10.1016/j.compag.2021.106125>
- Ahmad, A., Saraswat, D., & El Gamal, A. (2023). A Survey on Using Deep Learning Techniques for Plant Disease Diagnosis and Recommendations for Development of Appropriate Tools. *Smart Agricultural Technology*, 3, 100083. <https://doi.org/10.1016/j.atech.2022.100083>
- Ashwini, C., & Sellam, V. (2023). EOS-3D-DCNN: Ebola Optimization Search-Based 3D-Dense Convolutional Neural Network for Corn Leaf Disease Prediction. *Neural Computing and Applications*, 35(15), 11125–11139. <https://doi.org/10.1007/s00521-023-08289-3>
- Chakraborty, A., Kumer, D., & Deeba, K. (2021). Plant Leaf Disease Recognition Using Fastai Image Classification. *2021 5th International Conference on Computing Methodologies and Communication (ICCMC)*, 1624–1630. <https://doi.org/10.1109/iccmc51019.2021.9418042>
- Du, K., Jing, X., Zeng, Y., Ye, Q., Li, B., & Huang, J. (2023). An Improved Approach to Monitoring Wheat Stripe Rust with Sun-Induced Chlorophyll Fluorescence. *Remote Sensing*, 15(3), 693–867. <https://doi.org/10.3390/rs15030693>
- Gao, D., Li, M., Zhang, J., Song, D., Sun, H., Qiao, L., & Zhao, R. (2021). Improvement of Chlorophyll Content Estimation on Maize Leaf by Vein Removal in Hyperspectral Image. *Computers and Electronics in Agriculture*, 184, 106077. <https://doi.org/10.1016/j.compag.2021.106077>
- Görlich, F., Marks, E., Mahlein, A.-K., König, K., Lottes, P., & Stachniss, C. (2021). UAV-Based Classification of Cercospora Leaf Spot Using RGB Images. *Drones*, 5(2), 34–53. <https://doi.org/10.3390/drones5020034>
- Hossain, Md. I., Jahan, S., Al Asif, Md. R., Samsuddoha, Md., & Ahmed, K. (2023). Detecting Tomato Leaf Diseases by Image Processing Through Deep Convolutional Neural Networks. *Smart Agricultural Technology*, 5, 100301. <https://doi.org/10.1016/j.atech.2023.100301>
- Hua, S., Xu, M., Xu, Z., Ye, H., & Zhou, C. (2022). Multi-Feature Decision Fusion Algorithm for Disease Detection on Crop Surface Based on Machine Vision. In *Neural Computing and Applications* (Vol. 34, Issue 12, pp. 9471–9484). <https://doi.org/10.1007/s00521-021-06388-7>
- Javidan, S. M., Banakar, A., Vakilian, K. A., & Ampatzidis, Y. (2024). Tomato Leaf Diseases Classification Using Image Processing and Weighted Ensemble Learning. In *Agronomy Journal* (Vol. 116, Issue 3, pp. 1029–1049). <https://doi.org/10.1002/agj2.21293>
- Kundu, R., Dutta, D., Nanda, M. K., & Chakraborty, A. (2021). Near Real Time Monitoring of Potato Late Blight Disease Severity using Field Based Hyperspectral Observation. In *Smart Agricultural Technology* (Vol. 1, p. 100019). <https://doi.org/10.1016/j.atech.2021.100019>
- Lay, L., Lee, H. S., Tayade, R., Ghimire, A., Chung, Y. S., Yoon, Y., & Kim, Y. (2023). Evaluation of Soybean Wildfire Prediction via Hyperspectral Imaging. In *Plants* (Vol. 12, Issue 4, pp. 901–974). <https://doi.org/10.3390/plants12040901>
- Lei, S., Luo, J., Tao, X., & Qiu, Z. (2021). Remote Sensing Detecting of Yellow Leaf Disease of Arecanut Based on UAV Multisource Sensors. In *Remote Sensing* (Vol. 13, Issue 22, pp. 4562–4728). <https://doi.org/10.3390/rs13224562>
- Liao, K., Yang, F., Dang, H., Wu, Y., Luo, K., & Li, G. (2022). Detection of Eucalyptus Leaf Disease with UAV Multispectral Imagery. In *Forests* (Vol. 13, Issue 8, pp. 1322–1339). <https://doi.org/10.3390/f13081322>
- Mahum, R., Munir, H., Mughal, Z.-U.-N., Awais, M., Sher Khan, F., Saqlain, M., Mahamad, S., & Tlili, I. (2023). A Novel Framework for Potato leaf Disease Detection using an Efficient Deep Learning Model. In *Human and Ecological Risk Assessment: An International Journal* (Vol. 29, Issue 2, pp. 303–326). <https://doi.org/10.1080/10807039.2022.2064814>
- Ngugi, L. C., Abelwahab, M., & Abo-Zahhad, M. (2021). Recent Advances in Image Processing Techniques for Automated Leaf Pest and disease Recognition – A Review. In *Information Processing in Agriculture* (Vol. 8, Issue 1, pp. 27–51). <https://doi.org/10.1016/j.inpa.2020.04.004>
- Ouhami, M., Hafiane, A., Es-Saady, Y., El Hajji, M., & Canals, R. (2021). *Computer Vision, IoT and Data Fusion for Crop Disease Detection Using Machine Learning: A Survey and Ongoing Research*. Remote Sensing. <https://doi.org/10.3390/rs13132486>
- Qi, H., Wu, Z., Zhang, L., Li, J., Zhou, J., Jun, Z., & Zhu, B. (2021). Monitoring of Peanut Leaves Chlorophyll Content Based on Drone-Based Multispectral Image Feature Extraction. In *Computers and Electronics in Agriculture* (Vol. 187, p. 106292). <https://doi.org/10.1016/j.compag.2021.106292>

- Rahman, S. U., Alam, F., Ahmad, N., & Arshad, S. (2023). Image Processing Based System for the Detection, Identification and Treatment of Tomato Leaf Diseases. *Multimedia Tools and Applications*, 82(6), 9431–9445.
<https://doi.org/10.1007/s11042-022-13715-0>
- Shahi, T. B., Xu, C.-Y., Neupane, A., & Guo, W. (2023). Recent Advances in Crop Disease Detection Using UAV and Deep Learning Techniques. *Remote Sensing*, 15(9), 2450–2481.
<https://doi.org/10.3390/rs15092450>
- Srivastava, P. K., Gupta, M., Singh, U., Prasad, R., Pandey, P. C., Raghubanshi, A. S., & Petropoulos, G. P. (2021). Sensitivity Analysis of Artificial Neural Network for Chlorophyll Prediction using Hyperspectral Data. *Environment, Development and Sustainability*, 23(4), 5504–5519.
<https://doi.org/10.1007/s10668-020-00827-6>
- Tetila, E. C., Machado, B. B., Menezes, G. K., Da Silva Oliveira, A., Alvarez, M., Amorim, W. P., De Souza Belete, N. A., Da Silva, G. G., & Pistori, H. (2020). Automatic Recognition of Soybean Leaf Diseases Using UAV Images and Deep Convolutional Neural Networks. *IEEE Geoscience and Remote Sensing Letters*, 17(5), 903–907.
<https://doi.org/10.1109/lgrs.2019.2932385>
- Wang, Y., Chen, Y., & Wang, D. (2022). Convolution Network Enlightened Transformer for Regional Crop Disease Classification. *Electronics*, 11(19), 3174–3260.
<https://doi.org/10.3390/electronics11193174>
- Zamani, A. S., Anand, L., Rane, K. P., Prabhu, P., Buttar, A. M., Pallathadka, H., Raghuvanshi, A., & Dugbakie, B. N. (2022). Performance of Machine Learning and Image Processing in Plant Leaf Disease Detection. *Journal of Food Quality*, 2022, 1–7.
<https://doi.org/10.1155/2022/1598796>